Applied Catalysis B: Environmental 236 (2018) 490–500

Contents lists available at ScienceDirect

Applied Catalysis B: Environmental

journal homepage: www.elsevier.com/locate/apcatb

Ethanol and diethyl ether catalytic conversion over commercial alumina and lanthanum-doped alumina: Reaction paths, catalyst structure and coking

Gabriella Garbarino[a,b], Raam Prasath Parameswari Vijayakumar[a], Paola Riani[b,c], Elisabetta Finocchio[a,b], Guido Busca[a,b,*]

[a] Università degli Studi di Genova, Dipartimento di Ingegneria Civile, Chimica e Ambientale (DICCA), Laboratorio di chimica delle superfici e catalisi, Via Opera Pia 15, 16145 Genova, Italy
[b] INSTM, UdR di Genova, Via Dodecaneso 31, 16145 Genova, Italy
[c] Università degli Studi di Genova, Dipartimento di Farmacia (DIFar), Viale Cembrano 4, 16147 Genova, Italy

ARTICLE INFO

Keywords:
Alumina
Lanthanum doping
Ethanol dehydration
Diethyl ether cracking
Acidity

ABSTRACT

Commercial high-pore-volume alumina and La-doped aluminas have been characterized and tested as catalysts for ethanol conversion to ethylene and diethyl ether and for diethyl ether cracking. In order to go deeper on reaction paths and mechanisms, steady state, TPSR and static experiments in an IR cell were performed. It is established that ethylene forms from ethanol by two parallel ways: i) cracking of ethoxy groups that occurs already at low temperature, and ii) the parallel synthesis and cracking of DEE at intermediate temperatures. Coordination of diethyl ether on Lewis sites represents the first step in its decomposition path. Lewis bonded DEE first cracks to ethoxy species and ethylene gas, while ethoxy species in part crack to a second step to another ethylene gas molecule and in part (only at low temperature) can desorb as gaseous ethanol. Commercial low loading lanthanum-doped alumina contain dispersed La^{3+}-O^{2-} species mainly interacting with the most reactive defect, edge and corner sites of alumina nanocrystals. At higher loading (4 wt% La_2O_3) very small La_xO_y clusters also appear. Lanthanum doping slightly reduces the number of active sites for ethanol dehydration as well as for DEE cracking, thus reducing catalytic activity, but does not modify significantly selectivities and ethylene yields at high temperature. However, it also considerably reduces the amount of carbonaceous residues formed upon both reactions over the catalyst. Thus, La-doping is proposed as a way to improve the alumina catalyst stability in the process. Catalytic cracking of DEE at 673 K does not represent a good way to remove odorous and dense DEE vapours from air, due to the coproduction of small amounts of acetaldehyde together with ethylene.

1. Introduction

The conversion of bioethanol to (bio)ethylene has been industrially performed for several years. According to Morschbacker [1], the first commercial plant to produce ethylene from ethanol was built and operated, using an alumina catalyst, at Elektrochemische Werke GmbH at Bitterfeld in Germany in 1913. Several processes have been commercially developed and operated [2]. Even after steam cracking was established as the main technology to produce light olefins from oil cuts, and ethanol was mostly produced by ethylene hydration, still industrial plants producing ethylene from ethanol were active in some countries such as China [3]. The interest in bioethanol dehydration technology reappeared recently [4,5] to produce renewable ethylene (bioethylene), with the development of new processes such as IFPEN-Axens (Atol) [6], BP-Technip (Hummingbird) [7], Braskem [8], G.I. Dynamics [9] and Biochemtex [10]. In these processes, acid catalysts are generally used: alumina, silica-alumina, zeolites, heteropolyacids and phosphoric acid are mostly considered [1,2,4,5]. Ethylene yields in industrial conditions are very high (> 95%), with almost total ethanol conversion. Previous studies showed that the performances of γ-Al_2O_3 [2,5,11], although very good, are limited at low temperature by uncomplete conversion and diethyl ether synthesis, while at high temperatures by the co-production of small amounts of higher hydrocarbons [12–14]. An additional main point is represented by the growth of carbonaceous materials that may progressively deactivate the catalyst [14]. Thus, catalyst regeneration is needed every couple of months [5] and is pursued mainly by steaming at relatively high temperature. Both phenomena might be supposed to be due, at least in part, to acid-catalyzed

* Corresponding author at: Università degli Studi di Genova, Dipartimento di Ingegneria Civile, Chimica e Ambientale (DICCA), Laboratorio di chimica delle superfici e catalisi, Via Opera Pia 15, 16145 Genova, Italy.
E-mail address: Guido.Busca@unige.it (G. Busca).

https://doi.org/10.1016/j.apcatb.2018.05.039
Received 3 March 2018; Received in revised form 10 May 2018; Accepted 14 May 2018
Available online 25 May 2018
0926-3373/ © 2018 Elsevier B.V. All rights reserved.

overconversion of ethylene.

Over all acid catalysts, diethyl ether is the main product at low temperature and conversion. In fact, diethyl ether (DEE) can be manufactured industrially from ethanol dehydration over acid catalysts. Alumina is again the most cited catalyst in the literature and is applied in industrial processes [15,16]. In this case, ethanol conversion is limited to around 60–80% per pass, unconverted ethanol being separed and recycled. DEE process yield is near 90% with coproduction of small amounts of ethylene.

A debate still exists on the details of ethanol dehydration mechanism, DEE being a possible intermediate in the reaction [17,18]. Additionally, DEE and ethylene may also appear as byproducts in processes for the conversion of bioethanol to other chemicals, such as hydrogen by steam reforming, butenes, butadiene, acetone, etc., in particular when using alumina-supported or bifunctional catalysts [19,20]. DEE is also an odorous Volatile Organic Compound largely used as a solvent. Thus, the investigation of DEE cracking reaction is relevant not only in relation to the mechanism of ethanol conversion [18] but also as a possible way to abate DEE from air and reducing its smelling [21].

The improvement of alumina as a catalyst for DEE and/or bioethylene production may be attempted by doping, in particular to limit ethylene overconversion to higher hydrocarbons and coke, thus improving ethylene selectivity and catalyst stability. In a previous paper [22] we reported on the impregnation of a commercial "small pore-volume" γ-Al_2O_3 sample with lanthanum nitrate, producing 5 wt% La_2O_3-Al_2O_3 catalyst (calculated as wt_{La2O3}/wt_{Al2O3}). This material, although significantly less active than the corresponding pure alumina (γ-Al_2O_3) in converting ethanol, was an even slightly more selective catalyst towards ethylene at full ethanol conversion. On the other hand, lanthanum is reported to be a relevant additive to alumina in catalysts formulation: it improves alumina properties by increasing its mechanical strength [23], it stabilizes spinel-type alumina with respect to sintering and loss of surface area [24] and it activates alumina-supported metallic catalysts [25]. In particular, we found an interesting activation effects of lanthanum doping for alumina supported Ni catalysts applied to reactions useful in the environmental catalysis field, such as ethanol steam reforming and biomass tar steam reforming [26] as well as CO_2 methanation [27]. Thus, much interest is focused today on the preparation and characterization of La-containing aluminas [28–30]. Recently, Sasol commercialized La-containing aluminas powders [31]. In spite of this great interest, deep spetroscopic characterization studies of La_2O_3-Al_2O_3 systems are still very limited.

To go deeper on the chemistry of (bio)ethanol on oxide catalysts, as well as on the catalytic behaviour of lanthanum doped alumina, we investigated the conversion of both ethanol and diethyl ether over commercial γ-Al_2O_3 and La-γ-Al_2O_3 at 423–773 K with diluted ethanol feed at ambient pressure. In particular, we report here on the characterization of high pore-volume γ-Al_2O_3 and La-γ-Al_2O_3 (La_2O_3 ~ 1% and 4% wt), recently commercialized by Sasol, using XRD, skeletal IR, Field Emission Scanning Electron Microscopy (FE-SEM) as well as IR studies of surface hydroxy- groups, adsorbed pyridine and CO_2. Moreover, we investigated the effect of lanthanum addition on the behaviour of alumina as catalyst for ethanol dehydration to DEE and ethylene and of DEE cracking.

2. Experimental

2.1. Materials

The catalysts were commercial materials from Sasol, used without any further pretreatment. The notation used is the following: PTH for pure alumina Puralox TH 100/150, PL1 for Puralox TH 100/150/L1 and PL4 for Puralox TH 100/150/L4. The properties of these materials are summarised in Table 1.

Table 1
Samples notations and surface area.

Sample	$\%La_2O_3$ (wt_{La2O3}/wt_{CAT})[a]	S_{BET} [m^2/g_{CAT}][a]	$Å^2_{CAT}/at_{La}$	at_{La} /nm^2_{CAT}	Theoretical monolayer fraction[b]	$\%La_2O_3$ (wt_{La2O3}/wt_{CAT})[c]
PTH	0	146	–	0	0	0
PL1	1.20	151	344	0.29	0.06	1.5
PL4	4.0	155	104	0.96	0.18	5.5

[a] Data from the producer.
[b] Assuming 5.2 La atoms per nm^2 of alumina as the monolayer coverage.
[c] from EDX analysis.

2.2. Materials characterization

X-Ray diffraction patterns were recorded using Cu Kα radiation (λ = 0.15406 nm) by means of a Philips X'Pert diffractometer, in the 2θ angle range varying from 10° to 100° with a step of 0.02° and an acquisition time of 17 s for each step.

IR studies were performed using a Nicolet Nexus Fourier Transform instrument on compacted powder disks of 15–30 mg activated in vacuum at 773 K before adsorption experiments. CO_2 (30 Torr) was adsorbed at room temperature (r.t.) and spectra were recorded in the presence of the gas and after outgassing at room temperature and at increasing temperature. Pyridine (5 Torr) was put in contact with the catalysts for ten minutes and then outgassed at r.t. and upon increasing temperatures (373–773 K).

DR-UV–vis-NIR spectra were collected with a JASCO V570 instrument equipped with an integrating sphere.

SEM-EDX analysis were performed by a scanning electron microscope ZEISS SUPRA 40 VP, with a field emission gun as emitter. This instrument is equipped with a high sensitivity "InLens" secondary electrons detector to investigate morphology, with a solid state backscattered detectors to enhance compositional contrast and with a Energy Dispersive X-ray Spectrometer OXFORD "INCA Energie 450 × 3" to evaluate the composition of the overall samples and of the different constituting phases (EDXS).

2.3. Catalytic experiments

2.3.1. Steady state catalytic measures (steady state flow reactor study – SSFR)

Catalytic experiments were performed at atmospheric pressure in a tubular flow reactor (i.d. 6 mm) using 0.500 g catalyst (60–70 mesh sieved, thus achieving a ratio between the particle and internal reactor diameter near to 25) and feeding ethanol (99.8% assay, from Sigma Aldrich) in nitrogen with 12 h^{-1} WHSV (total flow rate of 80 cc/min). The carrier gas (nitrogen) was passed through a bubbler containing ethanol maintained at constant temperature (298 K) in order to obtain the desired partial pressures (7.9% ethanol/ 92.1% N_2). In the DEE experiments, the same catalysts weight have been used and a part of the carrier gas has been saturated with DEE at 293 K obtaining the following composition in the gas phase 4% DEE/96% N_2 achieving a WHSV of 12.8 h^{-1}. In both cases, the furnace temperature has been varied stepwise from 423 K to 773 K.

The outlet gases were analyzed by a gas chromatograph (GC) Agilent 4890 equipped with a Varian capillary column "Molsieve 5A/ Porabond Q Tandem" and TCD and FID detectors in series. In order to identify the compounds of the outlet gases, GC—MS Thermo Scientific with TG-SQC column (30 m × 0.25 mm × 0.25 μm) was used.

Reactant conversion is defined as usual:

$$X_R = (n_{R(in)} - n_{R(out)})/n_{R(in)} \text{ with R = DEE or EtOH}$$

While selectivity to product *i* is defined as follows:

$$S_i = n_i/(\nu_i(n_{R(in)} - n_{R(out)}))$$

where n_i is the moles number of compound *i*, and ν_i is the ratio of stoichiometric reaction coefficients.

2.3.2. Temperature Programmed Surface Reaction (TPSR)

Ethanol and diethyl ether Temperature Programmed Surface Reactions (EtOH-TPSR and DEE-TPSR, respectively) were carried out with a bed constituted by 0.043 g of the catalyst mixed with 0.127 g of sand (purchased from Sigma-Aldrich and calcined at 1073 K for 6 h prior to use) and using as reactant both ethanol (99.8%) and DEE (99.5%). The bed constituted by 0.170 g of sand resulted to be fully inactive in blank experiments in the same temperature range. For EtOH-TPSR, a mixture 2% ethanol / 98% N_2 with a total flow rate of 170 Nml/min was fed to the reactor, while temperature was raised from 373 K up to 773 K with a ramping rate of 5 K/min. For DEE-TPSR, a mixture 2% DEE/ 98% N_2 with a total flow rate of 170 Nml/min was fed to the reactor, while temperature was raised from 373 K up to 773 K with a ramping rate of 15 K/min. The outlet gases were collected online using a gas cell and an IR spectrometer (ThermoNicolet Instrument) and all components have been calibrated prior to TPSR experiments. Diagnostic bands at 1143 cm^{-1}, 1059 cm^{-1} and 951 cm^{-1} have been used for DEE, ethanol and ethylene respectively. Insight for acetaldehyde presence have been obtained by looking at the diagnostic band at 1750 cm^{-1}. Prior each TPSR experiment, an accurate background was collected with pure N_2 maintaining the exactly the same flow rate.

2.3.3. Ethanol and diethyl ether conversion in the infrared cell

Infrared studies of ethanol and diethyl ether conversion were performed in static conditions with a few Torr of vapours, i.e. ethanol or DEE, in the reaction cell, put into contact with a pure powder pressed disk of the catalyst previously activated by outgassing at 773 K. Both surface and gas phase IR spectra have been collected as a function of temperature (473–773 K). In all cases, a Nexus ThermoNicolet instrument was used (OMNIC software, DTGS detector, 100 scans). All the spectra are reported in common scale.

3. Results

3.1. Characterization of the fresh catalysts

In Table 1, data on surface area and composition coming from the producer are reported. EDX analysis of the samples matches with the one assessed by the produced even though a slight enrichment in La is observed in our analysis. The XRD patterns of the three samples (Fig. S1) present the diffractogram of γ-alumina, assumed to be a nearly cubic non-stoichiometric spinel [32]. No traces of other phases are observed even though in both cases the relative peak intensity is reduced. Interestingly, no shifts of (400) and (440) γ-Al_2O_3 peaks are observed suggesting that La did not enter in the Al_2O_3 lattice, as expected indeed. Skeletal IR spectra present the characteristic absorptions of spinel type alumina, with no modifications. La- containing samples in KBr pressed disks display, when compared to γ-Al_2O_3, two additional weak features at 1391 and 1509 cm^{-1}, typical of carbonate species (Fig. S2). FE-SEM – EDX analyses confirm a homogeneous distribution of Lanthanum over the alumina particles, as also reported by the supplier [31], without showing any significant La-rich particles (Fig. S3).

3.1.1. Surface characterization by IR spectroscopy

The IR spectra of the OH stretching region of the three samples after activation in vacuum at 773 K and 873 K are reported in Fig. 1, left. The spectrum of PTH shows sharp bands at 3768, 3727 and a doublet at 3682, 3675 cm^{-1}, with an additional weak shoulder near 3793 cm^{-1}, typical of the surface OHs of γ-Al_2O_3 [32–34]. The relative intensity of the overall massive absorption in the interval 3800–3620 cm^{-1} decreases in the order PTH > PL1 > PL4, with the ratio 1: ~ 0.75: ~ 0.5, for the samples outgassed at 773 K. The intensity of both higher and lower frequency components decreases significantly in the spectrum of PL1 and PL4, where the band near 3727 cm^{-1} becomes the predominant one and broadens too. A relatively broad component also appears at 3713 cm^{-1} which could be due either to a perturbed AlOH or to a LaOH group [35–38]. The effect of Lanthanum is roughly similar to that previously observed for impregnated samples prepared in our laboratory, starting from a different alumina sample [22]. The data show that Lanthanum addition, even at these relatively low loadings, modifies significantly the surface of alumina, reducing the amount of Al−OH hydroxyl groups, and producing new La−OH groups.

The IR spectra of the samples after activation at 773 K are also shown in the range 1700–1000 cm^{-1} in Fig. 1, right. It is evident that the presence of lanthanum decreases the intensity of absorption near the cut-off due to the skeletal vibration, which correspondingly shifts down from 1030 cm^{-1} for PTH to 995 cm^{-1} for PL1 and 980 cm^{-1} for PL4. This is due to the perturbation of the surface Al−O bonds [39,40] by lanthanum, taking into account that La is far heavier than aluminum and that La−O bonds absorb at lower frequencies than Al−O bonds.

The IR spectra of pyridine adsorbed on the three catalysts after outgassing at 373 K are reported in Fig. 2. As discussed elsewhere [33,41], the 8a mode bands at 1623 and 1614 cm^{-1} and the corresponding 19b mode bands at 1455 cm^{-1} (pronounced shoulder) and 1449 cm^{-1} are due to pyridine interacting with two different families of low coordination Al cations on the corners and on the edges (or, in any case, on defects) of the γ-Al_2O_3 crystals. The addition of La causes a decrease of the intensity of all these bands, indicating that the amount of Lewis acid sites is reduced. The relative intensity of the absorptions of Lewis bonded pyridine is 1:0.6:0.45 for PTH:PL1:PL4. On the other hand, the highest frequency component at 1623 cm^{-1} decreases more than the component at 1614 cm^{-1}. A rough estimate of the acidity amount reduction can be obtained by looking at the absorbance ratio of the maxima $\Delta A_{1623}/\Delta A_{1614}$; it is 0.82 for PTH, 0.68 for PL1 and 0.53 for PL4. This shows that the effect of lanthanum oxide species in decreasing the amount of Lewis acid sites is more pronounced for the strongest sites than for the weakest ones. In the spectrum recorded over sample PL4, a new 8a component clearly appears, sharp, at 1602 cm^{-1}, which could be attributed to pyridine adsorbed on lanthanum ions acting as weak Lewis acid sites, in rough agreement with results reported for pyridine adsorbed on other La-containing aluminas [22,42–44].

The IR spectra of the species arising from CO_2 adsorption on the three catalysts after brief outgassing at r.t. are compared in Fig. 3. The bands at 1654 cm^{-1}, 1443–1429 cm^{-1} and 1228 cm^{-1} observed upon adsorption of CO_2 on PTH are due to surface monohydrogencarbonate species (C═O asymmetric and symmetric stretching, and OH deformation, respectively [45]). The spectrum of the adsorbed species is similar but reduced in intensity in the case of PL1 sample. The bands of these species are also present in the case of the sample PL4. Looking at the intensity of the band at 1228 cm^{-1}, the intensity ratio for the samples PTH:PL1:PL4 is 1:0.5:0.3. In the case of the sample PL4, the bands of monohydrogencarbonates are further reduced in intensity, the higher frequency components being also shifted to lower frequencies (1622 and 1422 cm^{-1}) while new broad absorptions appear in the region 1500–1600 cm^{-1} (undefined) and 1400–1350 cm^{-1}. These new bands are likely associated to carbonate species, probably of the bidentate type, interacting with La−O bonds. It can be remarked that these features were not previously observed for impregnated samples prepared in our laboratory, starting from a different alumina sample, but with a very similar La surface loading [22].

3.2. Catalytic activity

3.2.1. Ethanol Temperature Programmed Surface Reaction (EtOH-TPSR)

Ethanol TPSR curves on the three catalysts are reported in Fig. 4. Over PTH alumina, ethanol conversion starts at 480 K with the production of DEE only. At 520 K also ethylene starts to be produced. DEE concentration grows progressively but its curve has an inflection point

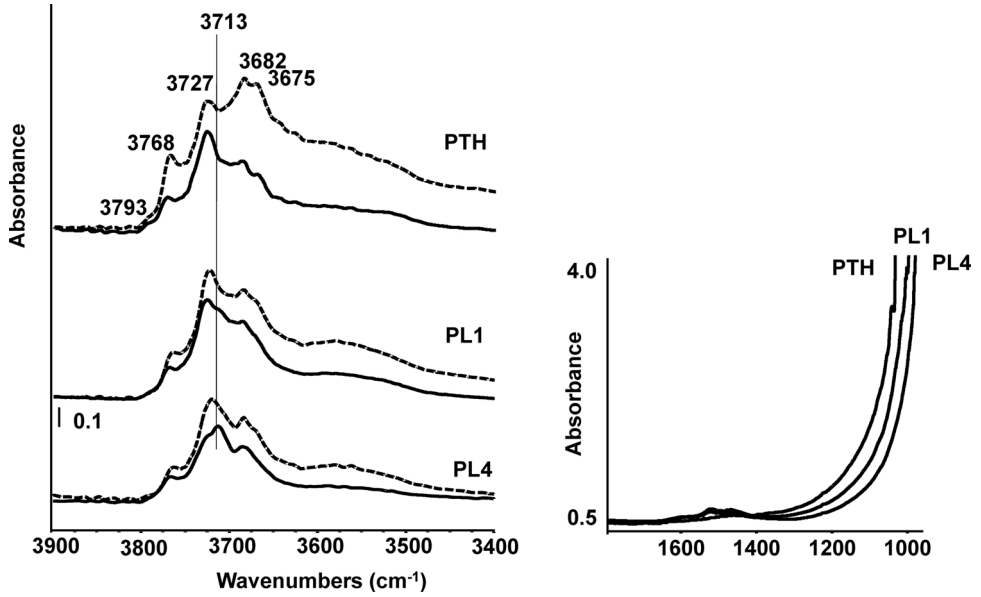

Fig. 1. IR spectra of the investigated catalysts after activation in vacuum at 773 K (dashed line) and 873 K (full lines) in the OH-streching region (left) and near the cut-off limit (right).

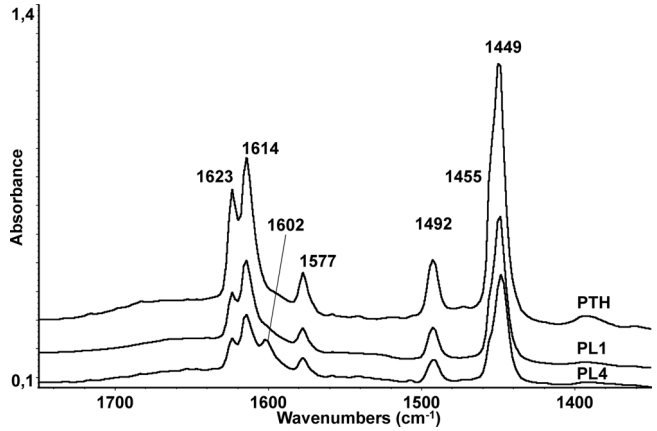

Fig. 2. IR spectra of pyridine adsorption for the investigated catalysts after activation at 773 K, contact with few torr of pyridine, outgassing at r.t. and evacuation at 373 K.

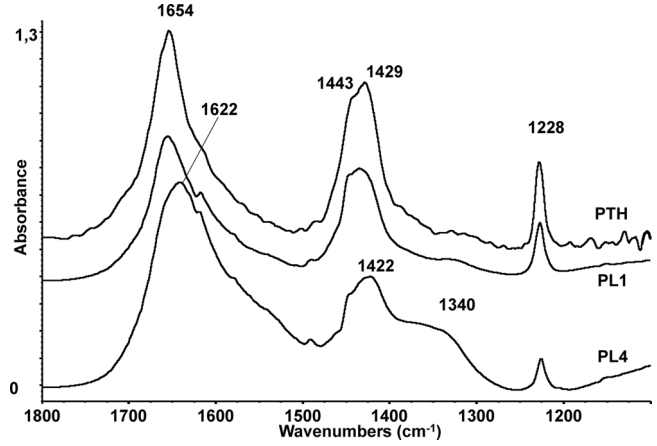

Fig. 3. IR spectra of CO_2 adsorption at r.t. (solid line) and after evacuation at the same temperature over the samples previously outgassed at 773 K.

around 540 K and peaks around 555 K. In the same temperature range, also the ethanol concentration curve has an inflection point, with an evident second component. DEE yield vanishes near 625 K, when ethanol conversion is still not complete. Near 660 K, ethanol is fully converted into ethylene. No other products are revealed in detectable quantity by online IR analysis. A careful look to the trends of ethanol, DEE and ethylene concentration curves suggests that the reaction pathway is quite complex. In the temperature range 480–520 K, ethanol is converted into DEE only, through reaction (1)

$$2\ CH_3CH_2OH \rightarrow (CH_3CH_2)_2O + H_2O \quad (1)$$

At increasing temperatures (520–555 K), ethanol is converted to both DEE (1) and ethylene (2)

$$CH_3CH_2OH \rightarrow H_2C{=}CH_2 + H_2O \quad (2)$$

by parallel reactions. In the range 555–630 K, these two reactions still occur with the possible addition of the DEE decomposition reaction to ethylene and ethanol

$$(CH_3CH_2)_2O \rightarrow CH_3CH_2OH + H_2C{=}CH_2 \quad (3)$$

Thus, producing the aforementioned inflection in the ethanol concentration curve. Above 630 K, ethanol converts essentially to ethylene only (maybe with small amounts of higher hydrocarbons), through reaction (2).

Over the PL1 catalyst, a similar behaviour is observed, even though it is slightly shifted at higher temperatures (10–15 K approx.). Ethanol conversion threshold and DEE yield peak are slightly shifted up by La doping, while the temperatures at which ethanol conversion and ethylene yield become complete is more markedly shifted up to near 675 K. The curves obtained on PL4 are similar to those observed on PL1 even if a further slight shift to higher temperature is observed. The ethylene/diethyl ether selectivity ratio at similar conversion is not significantly modified by lanthanum doping.

From the TPSR data, an estimate of apparent activation energy can be attempted, neglecting the transient nature of the experiment. Using ethanol conversion data in the range 450–520 K (low conversion, to approximately fulfill conditions of a differential reactor, and conditions where DEE and water are the only products) we calculated the activation energy for reaction (1) E_{ATT} = 94 kJ/mol. This value is in excellent agreement with literature data: 95–98 kJ/mol [46],

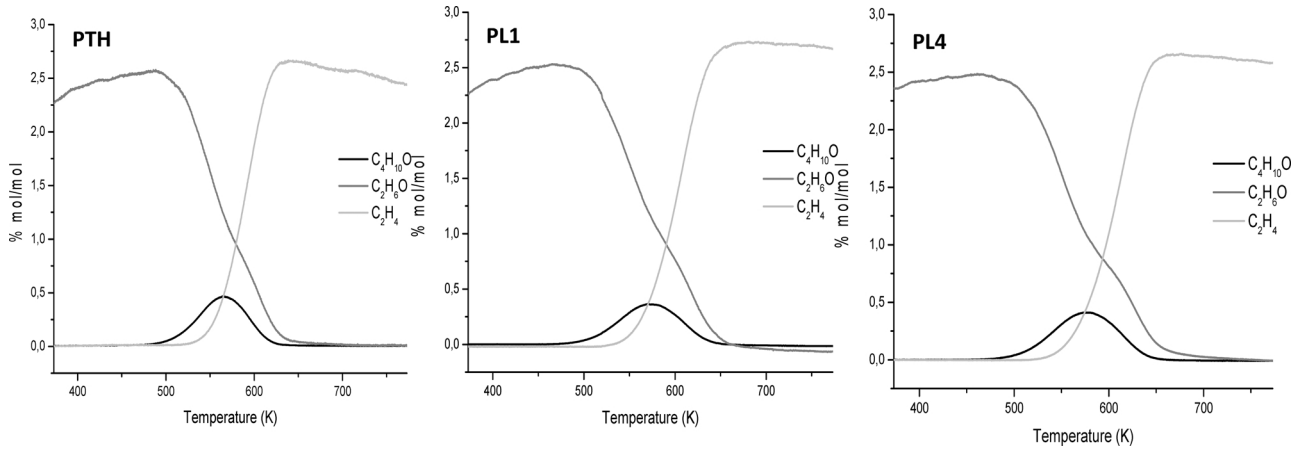

Fig. 4. Ethanol TPSR results on the investigated catalysts. Reaction conditions: catalysts mass 43 mg, total flow rate 170 ml/min (2% ethanol/98% N_2), temperature range 373–773 K, ramping rate 5 K/min.

105–120 kJ/mol [47] and recently 96–94 kJ/mol at 443–459 K and 86–64 kJ/mol 528–543 K, respectively [48]. These data also confirm that the experimental conditions chosen allow us to work in a kinetically controlled regime.

On the other hand, using ethylene formation rate in the range 520–555 K we can also obtain a rough assessment of the activation energy for ethylene formation directly from ethanol. The activation energy calculated from the Arrhenius plot on the ethylene formation rate (occurring through reaction (2)) is 182 kJ/mol. It compares well with the values reported by Lee and coworkers (170–175 kJ/mol at 443–473 K [46]) and by Wade (152–164 kJ/mol at 513–573 K [47]), and, roughly, with those reported in the recent paper of Lee [48] (155–167 kJ/mol at 443–459 K and 112–113 kJ/mol at 528–573 K).

As shown in Table 2, the addition of lanthanum in the catalysts poorly affects the activation energies values for both DEE and ethylene for the sample with the lowest loading (PL1, 1% La_2O_3), while a slight increase of both activation energies is detectable for PL4 samples.

3.2.2. Ethanol steady state flow reactor conversion (SSFR)

The data concerning the catalytic activity of the catalysts in ethanol conversion experiments are summarized in Table 3.

On the PTH sample, ethanol conversion starts to be observed above 423 K and approaches completeness (> 96%) at 573 K. DEE is first produced with 100% selectivity, its yield peaking at 523 K at 72.7% level, followed by a drop at higher temperatures. Ethylene selectivity is low (~14%) at 523 K and higher than 97% at total conversion (623 K and above). Indeed, ethylene yield achieves 98% at total conversion, being limited by the formation of ethane, propene and C4 hydrocarbons.

The behaviour of PTH sample in ethanol conversion experiments is closely similar, if tested exactly in the same conditions, to that observed, with the previously tested alumina [11,22] sample Puralox SBa200, which is characterized by a different morphology, with a lower pore volume but higher surface area. It should be consequently concluded that this sample PTH is a little more active (based on surface area) than the sample Puralox SBa200.

Table 2
Evaluation of apparent activation energy from EtOH-TPSR. The temperature range considered for calculation is also reported.

sample	T range [K]	E_{att} DEE formation [kJ/mol]	T range [K]	E_{att} Ethylene formation [kJ/mol]
PTH	440–520	94	520–570	182
PL1	447–531	99	531–588	182
PL4	463–532	120	524–577	199

Table 3
Ethanol conversion (X_{C2H5OH}) and selectivity to products (S_i) for ethanol conversion in steady state conditions in the flow reactor.

	T [K]	X_{C2H5OH}	S_{C2H4}	S_{C2H6}	S_{C3H6}	S_{C4}	S_{DEE}
PTH							
	423	1.0%	0.0%	0.0%	0.0%	0.0%	100.0%
	473	26.9%	0.6%	0.0%	0.0%	0.0%	99.4%
	523	84.6%	13.9%	0.0%	0.0%	0.2%	85.9%
	573	96.3%	92.3%	0.4%	0.0%	2.4%	4.9%
	623	100.0%	97.1%	0.4%	0.1%	2.3%	0.0%
	673	100.0%	98.1%	0.5%	0.1%	1.3%	0.0%
	723	100.0%	98.2%	0.6%	0.3%	0.9%	0.0%
	773	100.0%	98.3%	0.7%	0.4%	0.5%	0.0%
PL1							
	423	0.1%	0.0%	0.0%	0.0%	0.0%	100.0%
	473	18.4%	0.5%	0.0%	0.0%	0.0%	99.5%
	523	76.2%	5.6%	0.1%	0.0%	0.1%	93.6%
	573	92.1%	66.0%	0.3%	0.0%	1.0%	32.8%
	623	100.0%	97.4%	0.4%	0.0%	2.2%	0.0%
	673	100.0%	97.6%	0.4%	0.1%	1.7%	0.1%
	723	100.0%	97.5%	0.4%	0.3%	1.8%	0.0%
	773	100.0%	97.3%	0.7%	0.4%	1.6%	0.0%
PL4							
	423	0.5%	0.0%	0.0%	0.0%	0.0%	100.0%
	473	12.6%	0.5%	0.0%	0.0%	0.0%	99.5%
	523	69.2%	6.3%	0.0%	0.0%	0.3%	93.4%
	573	87.1%	59.9%	0.4%	0.0%	1.0%	38.8%
	623	100.0%	96.7%	0.5%	0.1%	2.6%	0.1%
	673	100.0%	96.9%	0.6%	0.1%	2.0%	0.4%
	723	100.0%	96.9%	0.4%	0.2%	1.7%	0.7%
	773	100.0%	96.3%	0.5%	0.4%	2.0%	0.7%

Ethanol conversion decreases progressively by increasing La loading at 473, 523 and 573 K, confirming the inhibiting effect of lanthanum. Selectivities to ethylene increase, as always, with conversion, without a significant effect of lanthanum loading. By looking to product selectivities at complete conversion, the addition of La does not clearly influences the selectivity and yield to ethylene. The differences observed are near the experimental error range for the measures.

3.2.3. Ethanol conversion in the IR cell

Ethanol conversion has also been investigated in the IR cell using pressed disks of pure catalysts. In Fig. 5, the spectra of the surface species adsorbed on the PL4 catalyst are reported upon this experiment, while the corresponding gas phase spectra are reported in Fig. 6. At 300 and 373 K the gas phase is constituted by ethanol vapour [49]; correspondingly, the spectrum of the surface, recorded at 300 K, contains

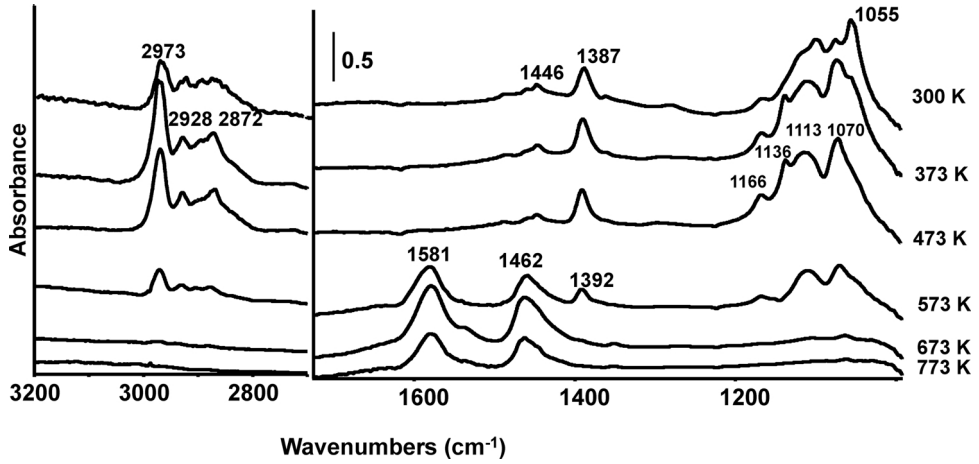

Fig. 5. IR spectra of surface species arising upon ethanol adsorption and reaction on activated PL4 catalysts as a function of temperature (300–773 K). (left) IR region 3200–2700 cm^{-1} and (right) 1700–1000 cm^{-1}.

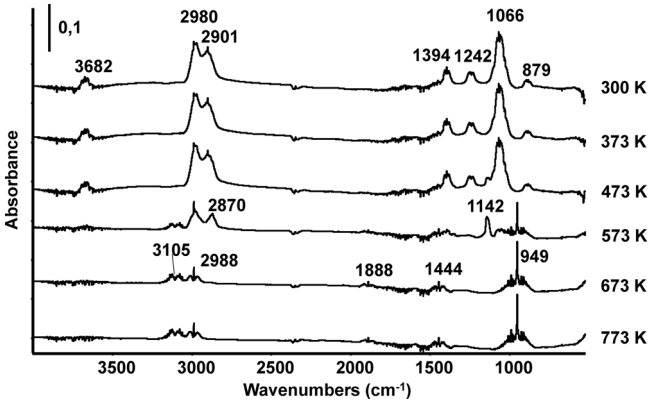

Fig. 6. IR spectra of the gas phase arising upon ethanol adsorption and reaction on PL4 catalysts as a function of temperature (300–773 K).

features of H-bonded ethanol (OH stretching at 1054 cm^{-1}) species, which have already disappeared at 373 K, together with those of ethoxy-groups, which resist heating at 473 K. The spectra recorded at 473 K over the three catalysts are compared in Fig. 7. In all cases, the bands near 2973, 2928, 2872 cm^{-1} are due to CH_x stretchings, while the maxima at 1446 cm^{-1} (δ_{as} CH_3) and near 1390 cm^{-1} (δ_{sym} CH_3) are due to deformation modes of the CH_3 group to which the CH_2 scissoring mode is superimposed. The band at 1166 cm^{-1} is essentially a CH_3 rocking mode also having a CO stretching character, while the bands in the envelop at 1200–1000 cm^{-1} are due to coupled C—O/C—C stretchings [50]. The only evident difference is due to an additional peak in the case of the PL4 sample at 1136 cm^{-1}, which is likely due to an ethoxy- group bonded to lanthanum ions.

By looking at the spectra upon temperature evolution (Figs. 5 and 6), over the PL4 sample the bands of surface ethoxides decrease in intensity at 573 K, when the feature attributed to La-ethoxide has already fully disappeared; even though, a complete disappearance of ethoxide is achieved only at 673 K. In parallel, two bands appear at 1581 and 1462 cm^{-1} and they can be assigned to surface acetate species (COO^- asymmetric and symmetric stretchings).

Looking at the gas phase, we see the formation of bands due to diethyl ether (C—O—C asymmetric stretching at 1142 cm^{-1} [51]) already, even if weak, at 473 K, strong at 573 K. Those features are absent at 673 K. Moreover, the bands of gaseous ethylene (CH_2 stretchings at 3105 and 2988 cm^{-1}; overtone of the CH_2 wagging mode at 1888 cm^{-1}, CH_2 scissoring mode at 1444 cm^{-1}, CH_2 wagging mode at 949 cm^{-1} [52]) appear at 573 K and are the only ones present at higher temperatures. These data show that, over PL4, ethanol starts to react at 473 K where only ethoxide species are observed at the surface, forming small amounts of DEE. At 573 K, ethanol is fully converted and DEE is present in large amounts in the gas, with ethylene also present, while the amount of surface ethoxy species is reduced. At 673 K ethylene yield is 100% in the gas and surface ethoxy groups have completely disappeared, leaving some residual surface acetate species.

The behaviour of the other two catalysts is not exactly the same (not shown): over PL1, DEE is formed in remarkable amounts at 473 K

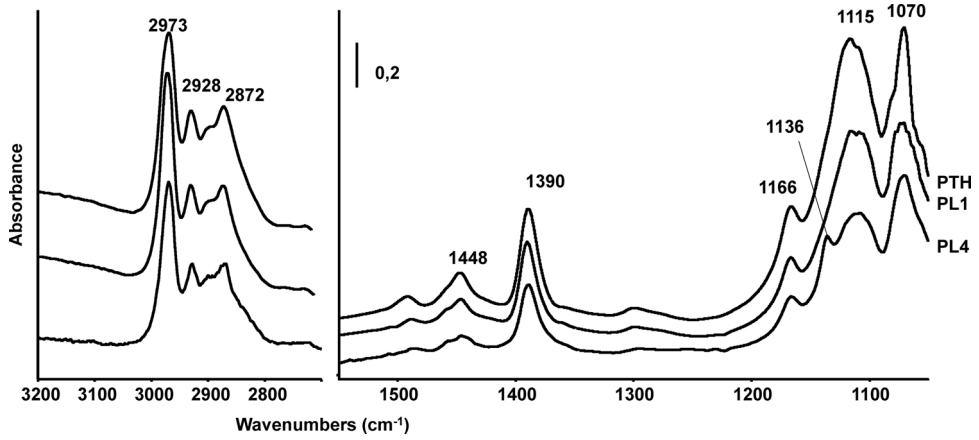

Fig. 7. IR spectra of surface species arising upon ethanol reaction at 473 K on PTH, PL1 and PL4 catalysts.

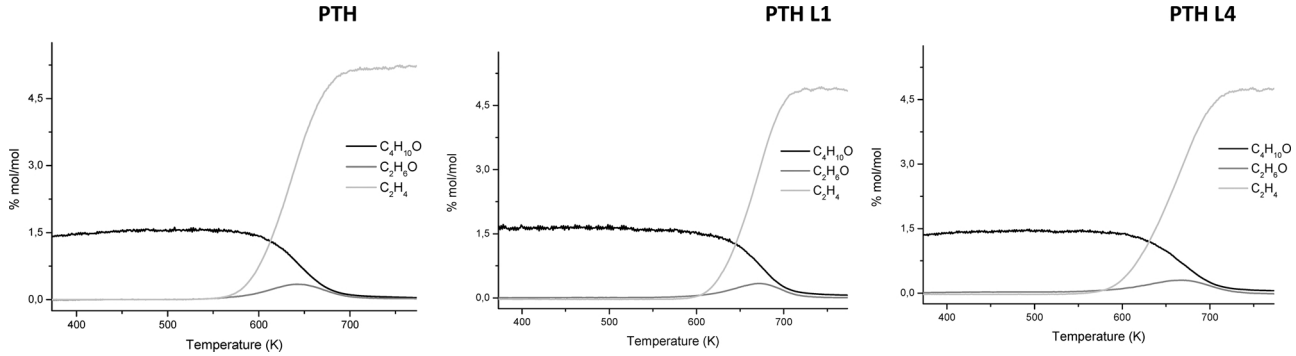

Fig. 8. DEE-TPSR results on the investigated catalysts. Reaction conditions: catalysts mass 43 mg, total flow rate 170 ml/min (2% DEE/98% N_2), temperature range 373–773 K, ramping rate 15 K/min.

(without any ethylene) while has already almost completely disappeared at 573 K, when also surface ethoxide species are almost absent, and ethylene is observed as main product in the gas phase. Over PTH, the situation is similar to what happens on PL1 but ethylene is already observed, in small amounts, at 473 K, and ethoxy groups have fully disappeared at 573 K.

Interestingly, gas-phase DEE is only observed when ethoxide groups are also present on the surface, in all cases.

3.2.4. Diethyl ether Temperature Programmed Surface Reaction (DEE-TPSR)

The curves of DEE-TPSR are reported in Fig. 8. Over PTH catalyst, DEE conversion starts around 560 K producing mostly ethylene together with small amounts of ethanol. Interestingly, very small amounts of acetaldehyde are observed too, along the all experiment, with a peak centered at 660 K. Full DEE conversion to ethylene is observed above 695 K. The amount of produced ethanol is always very low with a peak centered at 640 K. The curves on PL1 are similar but clearly shifted at higher temperatures: DEE conversion starts near 590 K and is complete near 723 K. Also in this case ethylene is by far the predominant product with the detection of small amounts of ethanol. The conversion of DEE seems to start on PL4 at intermediate conditions with respect to PTH and PL1. However, the temperature for full DEE conversion to ethylene as well as the peak in ethanol formation are slightly shifted at higher temperatures.

An estimate of activation energy for DEE conversion on the catalysts, evaluated at low conversion levels, indicates that a significant increase occurs for lanthanum containing catalysts (around 220 kJ/mol) than for pure alumina (190 kJ/mol). These values are, in any case, well higher than those measured for ethanol conversion and only slightly higher than those relative to direct ethylene conversion from ethanol, in agreement with a similar mechanism [53].

3.2.5. Diethyl ether steady state flow reactor conversion

DEE steady state conversion data over the three catalysts are reported in Table 4. DEE conversion is slightly higher at 423 K on La-containing catalysts than on pure alumina but, at higher temperatures, conversion on alumina becomes similar or higher than on La-containing catalysts, and becomes nearly total, over the three catalysts, at 623 K. Over alumina, ethylene is always the main product, with the coproduction of small amounts of ethanol at low conversion. However, acetaldehyde is also produced in significant amounts until conversion is far from complete. Over lanthanum containing catalysts, the selectivity to ethylene is higher than on alumina, and always well higher than selectivity to ethanol, with acetaldehyde selectivity lower than the one observed for alumina. Ethylene is produced with selectivities higher than 95% at nearly total DEE conversion, i.e. at $T \geq 623$ K, when ethane, propene and C4 hydrocarbons are co-produced in small amounts.

Table 4
Diethyl ether conversion (X_{DEE}) and selectivity to products (S_i) for DEE conversion in steady state conditions in the flow reactor.

	X_{DEE}	S_{CH2CH2}	S_{CH3CH3}	S_{C3H6}	S_{CH3CHO}	S_{C4}	S_{C2H5OH}
PTH							
423	0.0%	–	–	–	–	–	–
473	0.4%	tr	–	–	tr	–	tr
523	12.9%	57.5%	0	0	10.9%	0.8%	30.8%
573	67.3%	76.8%	0.3%	0.1%	7.9%	0.5%	14.3%
623	99.5%	90.4%	0	0.1%	7.3%	1.3%	0.9%
673	99.7%	93.9%	0.6%	0.2%	2.6%	2.4%	0.0%
723	99.9%	96.0%	0.4%	0.3%	0.9%	2.4%	0.0%
773	100.0%	97.4%	0.4%	0.4%	0.7%	1.2%	
PL1							
423	tr	0	0	0	tr	0	0
473	1.6%	tr	0	0	tr	0	0
523	12.4%	68.5%	0	0	4.0%	0.3%	27.3%
573	67.2%	83.1%	0.5%	0.0%	3.6%	0.1%	12.7%
623	99.9%	94.3%	1%	0.1%	4.4%	0.5%	0.0%
673	99.9%	96.5%	0.6%	0.1%	1.7%	1.0%	0.0%
723	99.9%	97.7%	0.4%	0.2%	0.5%	1.1%	0.0%
773	99.9%	98.4%	0.3%	0.3%	0.3%	0.6%	
PL4							
423	tr	0	0	0	tr	0	0
473	1.9%	tr	0	0	tr	0	0
523	12.7%	70.4%	0.0%	0.0%	5.5%	1.4%	22.8%
573	61.9%	81.5%	1.6%	0.0%	4.3%	0.4%	12.2%
623	99.8%	93.1%	1%	0.2%	5.2%	0.7%	0.0%
673	99.8%	95.8%	0.7%	0.0%	2.2%	1.1%	0.0%
723	99.6%	96.9%	0.8%	0.0%	0.7%	1.3%	0.0%
773	99.7%	97.6%	0.6%	0.3%	0.5%	0.9%	

Over all catalysts, the DEE conversion becomes significant, but is largely uncomplete, at $T < 623$ K. In all cases, DEE conversion is lower than the ethanol conversion, in the same temperature range.

Also starting from DEE, by-products are formed at high temperature thus limiting ethylene yield at the level of ~97%: they are the same observed from ethanol, i.e. ethane, propene and C4 hydrocarbons.

3.2.6. Diethyl ether conversion in the IR cell

In Fig. 9, the IR spectra of the surface species arising from the adsorption of DEE vapour on the PTH alumina sample are reported. In this experiment, DEE has been put into contact with the alumina sample, activated at 773 K in vacuum, and has been later outgassed at increasing temperature. The spectrum before outgassing shows two adsorbed species. One is similar to vapour phase DEE with the main band, due to C—O—C asymmetric stretching, split at 1142, 1137 cm^{-1} probably due to the existence of two conformers. These species disappear by outgassing at r.t., thus being very weakly bonded. The second one is characterized by the C—O—C asymmetric stretching band at 1104 cm^{-1}. It decreases much in intensity and shifts down to 1094 cm^{-1} by outgassing at r.t., but is stable by further outgassing at

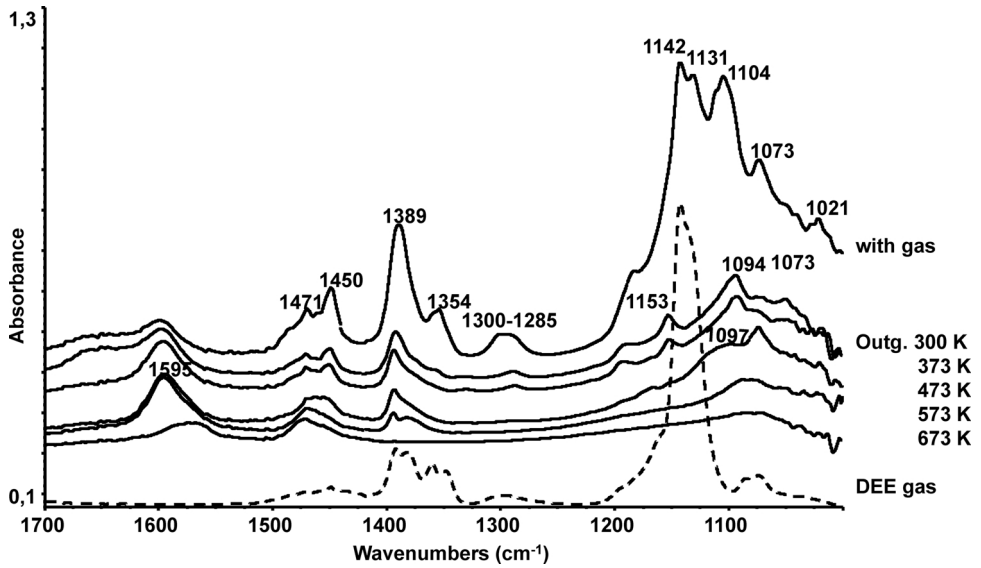

Fig. 9. IR spectra of surface species arising upon DEE adsorption on activated PTH catalyst as a function of outgassing temperature (300–773 K).

373 K. The spectrum observed is comparable to that reported for the $(C_2H_5)_2O$-$AlCl_3$ complex [54]. These molecular species disappear at 473 K leaving a spectrum which is closely similar to that is produced by ethanol adsorption and is assigned to ethoxy- groups. This spectrum weakens at 573 K and has completely disappeared at 673 K, when no more adsorbed species are found on the surface, except OH groups.

The spectra of the species observed in the DEE conversion experiment on the activated surface, i.e. in contact with the gas phase at increasing temperature are reported in Fig. 10. The spectra are less well-defined, and seem to be associated to the copresence of both molecularly adsorbed DEE and ethoxide species until 473 K, while only small amounts of ethoxide species are present at 573 K and 673 K.

Looking at the gas phase spectrum, DEE is stable at 473 K while it is almost completely transformed into ethylene at 573 K and fully converted at 673 K. Neither gas-phase ethanol nor acetaldehyde are observed.

The spectra recorded at r.t. after DEE adsorption on the three catalysts are similar and are all compatible with a molecular adsorption on Lewis acid sites (as reported for the interaction of DEE with $AlCl_3$ [55] and BF_3 [55]) and a reactive adsorption of DEE. The spectrum of the molecular species indicates that the adsorption shifts downward a little bit the C—O—C stretching mode to 1100 cm^{-1} on alumina and 1105 cm^{-1} on PL4 and PL1. The evolution observed on PL1 and PL4 is very similar to that described for PTH (Fig. 11).

3.2.7. Characterization of spent catalysts

After the catalytic experiments, both for ethanol and DEE conversion, the colour of the three catalysts is markedly darkened. However,

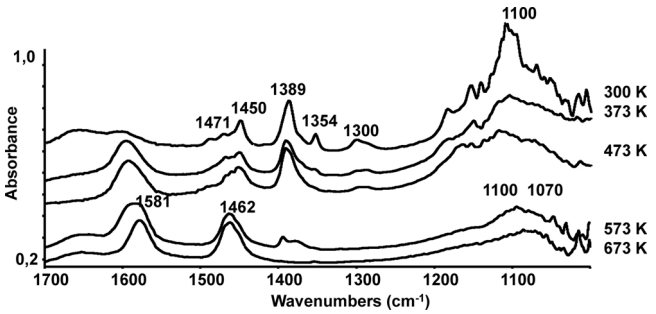

Fig. 10. IR spectra of surface species arising upon DEE adsorption and reaction on activated PTH alumina catalyst as a function of temperature (300–773 K).

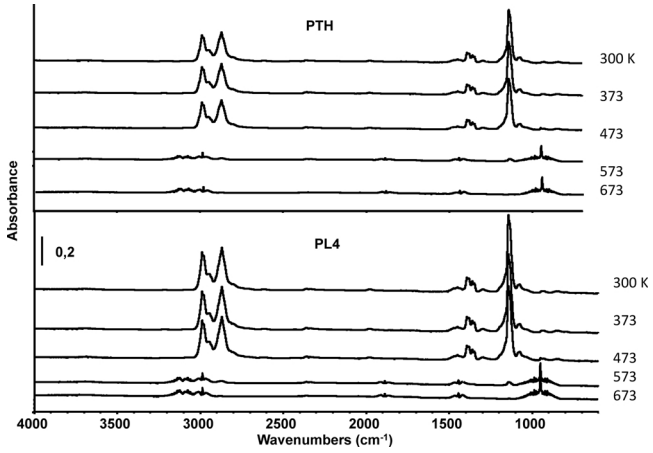

Fig. 11. IR spectra of the gas phase arising upon DEE adsorption and reaction on PTH alumina catalyst as a function of temperature (300–773 K).

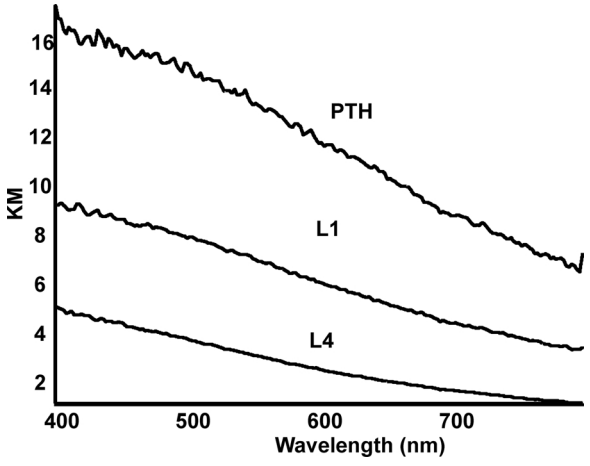

Fig. 12. DR-visible spectra of the catalysts after the catalytic experiments of DEE cracking.

the darkest samples are always those of pure alumina while the PL4 samples are always the clearest. This is confirmed by vis visible spectra (see Fig. 12 for the samples spent after DEE cracking experiments). It is

confirmed that the absorption of the PL4 sample is the weakest while that of pure alumina is the strongest. In all cases, the spectrum presents a continuous absorption growing towards lower wavelengths, without any maxima in the region of $\lambda > 250$ nm. The spectra are similar to those reported for graphite and coal samples [56] while they significantly differ from those of coke formed on zeolites upon ethanol conversion [14] as well as from those characteristic of carbon nanotubes [57]. In those cases, maxima are present in the visible region likely associated to the molecular nature of those species. In our case, the spectrum suggests a disordered graphite-like structure for carbon deposits.

The amount of carbon residues can be roughly evaluated by the weight of the spent catalytic beds. After the DEE cracking experiment the amount of carbon formed over the PTH alumina catalyst is around 9% wt_C/wt_{CAT}, while it decreases to 5.2% for PL1 and 2.5% for PL4. Analogous results are observed after the ethanol conversion experiments.

4. Discussion

4.1. Reaction paths of ethanol and diethyl ether conversion on alumina

The study of ethanol conversion on the PTH alumina sample confirms previous data showing the high activity of γ-Al_2O_3 in the conversion of ethanol producing diethyl ether (1) and ethylene (2), depending mostly on the reaction temperature.

It seems interesting to remark that the γ-Al_2O_3 sample used here is more active in terms of activity per surface area than the one previously used [11,22]. Data coming from the producer [58] indicate that the present Puralox TH 100/150 sample has lower surface area but much larger pore volume than the sample previously used by us (Puralox SBa200) and is also characterized more by prismatic than by lamellar particles. This could indicate that the main basal planes of lamellar γ-Al_2O_3 particles coming from boehmite precursor should not be the most involved in catalysis. It seems likely that edges involving non-basal planes could be the most active in the reaction.

The reaction (1) producing DEE starts at 473–523 K and is predominant until 523 K–600 K, depending on conditions (TPSR vs SSFR). We can take into account that TPSR experiments have been performed with lower ethanol partial pressure (2% with respect to 7.9% for SS) but with much higher space velocity (300 h^{-1} with respect to 12 h^{-1} for SS) than SSFR. The far higher contact time is likely the main reason why the reactions are slightly faster in SSFR than in TPSR.

At higher temperatures, ethylene becomes the predominant product, with very high yield at $T > 623$ K; this is limited by the production of small amounts of higher hydrocarbons. However, TPSR data show that ethylene is also formed at relatively low temperature, when reaction (2) is parallel to reaction (1). At intermediate temperatures, ethylene is likely both produced directly from ethanol (reaction (2)) and from diethyl ether cracking through reaction (3) followed again by reaction (2). The infrared study shows the formation of ethoxy- groups as the main surface species, which start to be unstable in conditions where diethyl ether is formed in the gas phase, and disappear when ethylene becomes the predominant product. These results suggest that these species can be intermediate for the production of both products, DEE production needing significant concentration of ethanol in the gas phase or adsorbed in an undissociated form. The mechanism of DEE formation would imply the reaction of adsorbed ethoxide species with weakly adsorbed, probably H-bonded, ethanol species, while the main way to ethanol would imply the decomposition/elimination of ethoxide species.

DEE conversion starts and grows at higher temperatures than ethanol conversion in the three experiments (TPSR, steady state activity, static conversion in the infrared cell). This indicates that the reaction rate for DEE cracking is slower at low temperature than the reaction of intermolecular dehydration of ethanol to diethyl ether, in agreement with the detection of DEE in relevant yield as a product of ethanol dehydration. On the other hand, well higher activation energy is measured for DEE cracking than for DEE formation (170 kJ/mol with respect to 94 kJ/mol on alumina) in the experiments. Thus, the endothermic DEE cracking becomes faster than DEE formation (as it is obvious indeed) at higher temperatures and DEE disappears among the ethanol dehydration products. However, the temperature range where conversion is incomplete for both reactants is the same, thus also justifying the formation of small amounts of ethanol from DEE too.

TPSR data show that ethylene is formed from ethanol even before it is formed from DEE, thus confirming that, also at low temperature, reaction (2) occurs parallel to reaction (1) and, at higher temperature, also parallel to reaction (3). Thus, ethylene is formed at least in part, by monomolecular dehydration of ethanol also at low temperatures.

According to IR spectroscopy studies, DEE adsorbs molecularly on the Lewis acid sites of alumina, with a decrease of the C—O—C stretching frequency. Its conversion starts to be significant near 560 K in TPSR experiments and near 500 K in SSFR experiments. Ethylene is the main product of DEE cracking with small amounts of ethanol formed only in the range $T < 623$–673 K, i.e. in the temperature region where conversion of ethanol itself is still incomplete. In IR experiments, surface ethoxy- groups are observed to form from adsorbed DEE. This indicates that reaction (3) certainly occurs with ethanol readsorbing at least in part as ethoxy groups. However, in the meantime reaction (2) already occurs fast, thus converting the produced ethanol to ethylene too. This is the reason why the ethylene/ethanol product ratio from DEE is always well higher than 1. This confirms that reaction (2) is a real step, i.e. that intramolecular ethanol dehydration actually occurs also without the intermediacy of DEE, even at moderate temperature. It is concluded that, starting from ethanol, reactions (1) and (2) are at least in part parallel, also at low temperature, although the sequence of reactions (1) + (3) + (2) is also possible.

On the other hand, it is confirmed that the formation of diethyl ether from ethanol is limited by the availability of the reactant in the gas phase, and tends to vanish when ethanol is predominantly adsorbed in the form of ethoxide species. When vapour phase ethanol is lacking and temperature is sufficiently high, ethoxy groups convert selectively into gas phase ethylene. Thus, ethylene/DEE selectivities are mostly governed by conversion and temperature.

Conversely, diethyl ether cracks at low temperature producing ethylene and ethoxy groups in equilibrium with vapour phase ethanol, but when temperature is sufficiently high only ethylene is produced. This picture roughly agrees with the data of DeWilde and Bhan [53].

Both starting from ethanol and from diethyl ether, byproducts form at total conversion limiting ethylene yield to values near 97% in our conditions: they are ethane, propene and butenes. On the other hand, even if we do not find catalyst deactivation in one day experiments, the growth of carbonaceous matter over the catalyst is evident and considerable. Thus, deactivation is expected in longer time on stream experiments (as reported in the literature [5]), and intermittent regeneration steps are needed for prolonged activity.

4.2. Effect of La-doping on the surface properties of γ-Al_2O_3

The characterization data reported above show that the addition of small amounts of lanthanum strongly modifies the surface structure of γ-Al_2O_3. Taking into account that the theoretical monolayer for La_2O_3/Al_2O_3 system was evaluated in previous papers [59,60] to be a little more than 5 La atoms per nm^2, the amount of lanthanum loaded (Table 1) can be evaluated to correspond to a small fraction of the theoretical monolayer in both cases of PL1 and PL4.

In spite of this, the overall intensity of the complex absorption due to the surface hydroxyl groups decreases much more than expected for the fractional coverage of the surface by increasing La, with a more pronounced decrease of both the highest and lowest frequency components. This suggests that, as also shown for deposition of other

species like silicates and Ni oxide [61], this phenomenon is quite selective, occurring predominantly on specific positions. Surface OH's of alumina may be exchanged or reacting with $La^{3+}O^{2-}$ couples becoming neutralised. In the central spectral OH stretching region, a new component seems to increase, centred at 3713 cm^{-1}, possibly associated to LaOH groups.

The spectra of adsorbed pyridine show Lewis acidity in all samples, without any significant Brønsted acidity. Again, the intensity of the bands of Lewis bonded pyridine decrease by La addition much more than expected by the fractional coverage of the surface, suggesting again that the alumina's Lewis acid sites occupy a moderate fraction of its surface, and that La addition acts as a selective poisoning of the Lewis sites. Interestingly, the effect of lanthanum oxide species on the strongest Lewis acid sites is more pronounced than on the weakest ones. Highly uncoordinated Al^{3+} Lewis acid sites, likely associated to quite reactive O^{2-} oxide anions, possibly act as preferential anchoring sites for La^{3+} O^{2-} couples, whose basic O^{2-} counterparts "poison" them. Additionally, the feature of a new family of La^{3+} Lewis acid sites are apparent in the case of the PL4 sample.

Also in the case of CO_2 adsorption, the formation of monohydrogencarbonate species is evident in all sample but their amount decreases by La doping more than expected by the fractional coverage. Additionally, new sites appear producing carbonate species.

Thus, a rough evaluation of the intensity of the bands of adsorbed probe molecules indicates that a coverage of 6% of the alumina surface (PL1 sample) results in killing of 25 % of the surface OH's, 40% of all Lewis sites, 54% of the strongest Lewis sites and of 50% of surface nucleophilic centers adsorbing CO_2. The coverage of 19% of the surface kills 50% of the surface OH's, 55% of all Lewis acid sites including 72% of the strongest Lewis acid sites, and 70% of nucleophilic sites.

The overall picture suggests that the dispersion of lanthanum and the accompanying oxide ions is good but occurs only over part of the most reactive sites of the alumina surface, i.e. surface defects, edges and corners of alumina nanocrystals. Only on PL4 very small La_xO_y clusters form (not detectable with FE-SEM), responsible for specific OH sites, Lewis acid and basic sites. In any case, the formation of massive lanthanum-containing structures, such as $LaAlO_3$, is excluded in the two samples investigated here. On the other hand, the comparison of the PL4 properties with that of the previously studied 5LaA sample [22], home-made prepared by impregnation of a slightly different alumina support with a very similar loading, shows worst dispersion of lanthanum species in the commercial sample than in the home-made one. This is deduced by the appearance, in the case of the commercial PL4 sample, of La_xO_y "clusters" with specific acido-basic sites.

4.3. Effect of La-doping on the catalytic properties of γ-Al_2O_3

The effect of La loading, also at these low amounts, significantly reduces the catalytic activity in ethanol conversion, which is in agreement with the assignment of the catalytic activity to both Al^{3+} strong Lewis acid sites and Al—OH surface hydroxyl groups that, as discussed previously [11], both allow the production of reactive surface ethoxide species. The evaluation of the activation energy for ethanol conversion to DEE indicates that it does not change for PL1, while increasing a little bit for PL4. Also the ethylene/DEE selectivity ratio does not change significantly with lanthanum amount. This shows, in agreement with pyridine adsorption experiments, that the number of active sites is mostly affected by lanthanum doping, more than their quality. It seems interesting to remark that the ratios of ethanol conversions at 473 K (see Table 3) for the three catalysts PTH:PL1:PL4 is 1:0.68:0.47 is surprisingly similar to the intensity ratios of the absorptions of Lewis bonded pyridine, which is 1:0.6:0.45. The slight increase in activation energy for ethanol conversion might be associated to the preferential poisoning of the strongest and more active Lewis sites, as discussed for pyridine adsorption.

The catalytic activity of the commercial PL4 sample studied here is significantly higher than that of the impregnated 5LaA sample studied in our previous work [22], in spite of the same surface coverage and the lower surface area. However, as said, also the high pore volume starting alumina studied here Puralox TH 100/150 is more active per surface area than the previously studied lower pore volume alumina Puralox SBa200. As said, IR spectroscopy data show for PL4 catalyst the presence of specific features attributed to small La_xO_y "clusters", that were not found over the previous 5LaA sample. These data suggest that the sample 5LaA we previously prepared by impregnation of Puralox SBa200 presents a better dispersion of lanthanum over the more active Lewis acid sites of alumina than the commercial PL4 sample. On the other hand, the ethylene yield at high conversion observed for PL4 (~97%) is slightly lower than that measured for 5LaA (~98%), and is not better than that observed for the present pure alumina (~98%). Even if these differences are quite repeatable, they are near the measurement error. It is difficult to conclude, from these data, whether La-doping can produce more selective catalysts for ethylene production.

The data indicate that lanthanum also reduces the activity of alumina for DEE cracking to ethylene and ethanol and to ethylene only. However, the effect of lanthanum here is weaker, and influences more the ethanol/ethylene product ratio at partial conversion. IR spectroscopy suggests that the preliminary interaction of DEE with the catalyst surfaces occurs through Lewis bonding on Lewis acid sites, producing first ethoxy groups and gas-phase ethylene. In these conditions, ethoxy-groups can either desorb as ethanol, or decompose to a second ethylene molecule (plus water). Thus, also in this case Lewis acidity is the key property for the reaction, the amount of sites being reduced by the loading of lanthanum, but a participation of surface basic sites in the cracking step can partially balance this effect.

However, it has been observed, that lanthanum favours the production of acetaldehyde at low temperature and moderate conversion, which is observed, however, also on pure alumina. Interestingly, we do find acetaldehyde from ethanol in the same conditions, neither on pure alumina nor on La-doped alumina. Additionally we do not find acetaldehyde from DEE at high temperature. The formation of acetaldehyde from DEE is thermodynamically possible, at least in small amounts, with different reaction stoichiometries. It is evident in any case that catalytic cracking of DEE producing acetaldehyde is certainly faster, over these catalysts, than ethanol dehydrogenation to acetaldehyde. In any case, the detection of acetaldehyde from DEE cracking represents a drawback in the possible use of cracking reaction as a technique to abate odorous DEE from polluted air.

On the other hand, we have observed that the presence of lanthanum, even in these small amounts, significantly reduces the amount of carbonaceous matter formed on the surface of alumina upon conversion of both ethanol and DEE. Even if we do not find any deactivation by coking in the one-day experiments we performed, it seems likely that the property of lanthanum to reduce coking can result in increased stability of La-doped alumina for ethanol conversion to both DEE and (bio)ethylene in practical industrial conditions.

5. Conclusions

The conversion / cracking, of ethanol and diethyl ether has been studied over a commercial large pore γ-Al_2O_3 and over commercial La-doped γ-Al_2O_3 samples (1–4%wt La_2O_3). The main conclusions of the work are the following:

1 Diethyl ether forms from ethanol at partial conversion with yields of the order of > 70% over all samples, while yields over 97% in ethylene are obtained over all samples at high temperature (> 600 K).
2 Diethyl ether cracks, mainly to ethylene and water above 600 K, while also some ethanol is formed at partial conversion in the range 400–600 K. However acetaldehyde is also formed in non-negligible amounts, upon DEE cracking, together with other hydrocarbons.

3 The data confirm that ethylene can be obtained both by diethyl ether cracking and also directly from ethanol via “monomolecular” cracking of ethoxy groups. Monomolecular dehydration of ethanol starts at lower temperatures than DEE cracking, thus being parallel to both DEE formation and DEE cracking. At higher temperature and conversion, ethylene is formed exclusively by monomolecular dehydration.
4 Ethoxy groups are intermediates in both diethyl ether synthesis and ethylene production from ethanol.
5 Coordination of diethyl ether on Lewis sites represents the first step in its decomposition path. Lewis bonded DEE first cracks to ethoxy species and ethylene gas, while ethoxy species in part crack in a second step to another ethylene gas molecule and in part (only at low temperature) can desorb as ethanol gas.
6 Catalytic cracking of DEE at 673 K over these catalysts cannot be a good way to remove odorous and dense DEE vapours from air, because of the coproduction of small amounts of acetaldehyde.
7 Commercial lanthanum-doped aluminas contain well dispersed La^{3+}-O^{2-} species first mostly interacting with the most reactive defect, edge and corner sites of alumina nanocrystals, while at higher loading (4%) very small La_xO_y clusters appear. In any case, lanthanum-rich phases (e.g. $LaAlO_3$) do not exist over these materials.
8 Lanthanum doping slightly reduces the number of active sites for ethanol dehydration as well as for DEE cracking, thus slightly reducing catalytic activity. However, it also significantly reduces the amount of carbonaceous residues formed upon both reactions over the catalyst, thus forming promising catalysts for prolonged time-on-stream application in ethanol conversion processes to DEE and to ethylene.
9 Doping alumina with lanthanum is proposed as a way to improve stability of alumina catalysts for the synthesis of bioethylene from bioethanol.

Acknowledgements

The authors acknowledge Sasol to supply the samples used in the present investigation. The authors would also like to acknowledge Veronica Ottonello that contribute to this work during the development of her bachelor thesis by carrying out a part of the experiments here reported.

Appendix A. Supplementary data

Supplementary material related to this article can be found, in the online version, at doi:https://doi.org/10.1016/j.apcatb.2018.05.039.

References

[1] A. Morschbacker, J. Polym. Rev. 49 (2009) 79–84.
[2] Y.C. Hu, Olefin processes, in: J.J. McKetta (Ed.), Chemical Processing Handbook, 1993, pp. 768–819.
[3] Zi Gao, Adsorption and catalysis, in: R.R. Xu, Zi Gao, Y. Xu (Eds.), Progress in Zeolite Science: A China Perspective, World Scientific, 1995, p. 151.
[4] D. Fan, D.-J. Dai, Ho-S. Wu, Materials 6 (2013) 101–115.
[5] A. Mohsenzadeh, A. Zamani, M.J. Taherzadeh, ChemBioEng Rev. 4 (2017) 75–91.
[6] https://www.axens.net/news-and-events/news/322/axens-total-and-ifpen-launch-atol-an-innovative-technology-for-bio-ethylene-production-through-dehydration-of-bio-ethanol.html#.Wh1qOFXiZ0w.
[7] http://www.technip.com/en/press/technip-completes-acquisition-hummingbird%C2%AE-technology-bp-chemicals-limited.
[8] http://www.chemicals-technology.com/projects/braskem-ethanol/.
[9] http://www.gidynamics.nl/ethanol-to-ethylene.
[10] http://www.biochemtex.com/en/sustainable-chemistry/bio-ethylene.
[11] T.K. Phung, A. Lagazzo, M.Á. Rivero Crespo, V. Sanchez Escribano, G. Busca, J. Catal. 311 (2014) 102–113.
[12] T.K. Phung, C. Herrera, M.Á. Larrubia, M. García-Diéguez, E. Finocchio, L.J. Alemany, G. Busca, Appl. Catal. A: Gen. 483 (2014) 41–51.
[13] G. Garbarino, I. Travi, M. Pani, M.M. Carnasciali, G. Busca, Catal. Commun. 70 (2015) 77–81.
[14] T.K. Phung, L. Proietti Hernandez, A. Lagazzo, G. Busca, Appl. Catal. A: Gen. 493 (2015) 77–89.
[15] M. Sakuth, T. Mensing, J. Schuler, W. Heitmann, G. Strehlke, D. Mayer, Ethers, aliphatic, Ullmann’s Encyclopedia of Industrial Chemistry, Wiley-VCH Verlag GmbH & Co. KGaA, Weinheim, 2012, pp. 437–438.
[16] W. Widayat, A. Roesyadi, M. Rachimoellah, Int. J. Sci. Eng. 4 (2013) 6–10.
[17] J.F. DeWilde, H. Chiang, D.A. Hickman, C.R. Ho, A. Bhan, ACS Catal. 3 (2013) 798–807.
[18] T.K. Phung, G. Busca, Chem. Eng. J. 272 (2015) 92–101.
[19] A. Limayem, S.C. Ricke, Prog. Energy Combust. Sci. 38 (2012) 449–467.
[20] M. Balat, Energy Convers. Manag. 52 (2011) 858–875.
[21] J.O. Chae, S.I. Moon, H.S. Sun, K.Y. Kim, V.A. Vassiliev, E.M. Mikholap, KSME Int. J. 13 (9) (1999) 647–655.
[22] G. Garbarino, C. Wang, I. Valsamakis, S. Chitsazan, P. Riani, E. Finocchio, M. Flytzani-Stephanopoulos, G. Busca, Appl. Catal. B: Environ. 200 (2017) 458–468.
[23] S. Kang, D. Lee, S. Kwon, Aerosp. Sci. Technol. 46 (2015) 197–203.
[24] P. Alphonse, B. Faure, Microporous Mesoporous Mater. 196 (2014) 191–198.
[25] L.J. France, X. Du, N. Almuqati, V.L. Kuznetsov, Y. Zhao, J. Zheng, T. Xiao, A. Bagabas, H. Almegren, P.P. Edwards, Appl. Petrochem. Res. 4 (2014) 145–156.
[26] G. Garbarino, C. Wang, I. Valsamakis, S. Chitsazan, P. Riani, E. Finocchio, M. Flytzani-Stephanopoulos, G. Busca, Appl. Catal. B: Environ. 174 (2015) 21–34.
[27] G. Garbarino, D. Bellotti, P. Riani, L. Magistri, G. Busca, Int. J. Hydrogen Energy 40 (2015) 9171–9182.
[28] S.J. Smith, B. Huang, C.H. Bartholomew, B.J. Campbell, J. Boerio-Goates, B.F. Woodfield, J. Phys. Chem. C 119 (2015) 25053–25062.
[29] J. Yang, Q. Wang, T. Wang, Y. Liang, RSC Adv. 6 (2016) 26271–26279.
[30] K. Patel, V. Blair, J. Douglas, Q. Dai, Y. Liu, S. Ren, R. Brennan, Sci. Rep. 7 (2017) 39946.
[31] Doped Aluminas, http://www.sasolgermany.de/fileadmin/doc/alumina/0271.SASBR-Inorganics_Siral_Siralox_WEB.pdf.
[32] G. Busca, Catal. Today 226 (2014) 2–13.
[33] G. Busca, Adv. Catal. 57 (2014) 319–404.
[34] K.H. Hadjiivanov, Adv. Catal. 57 (2014) 99–318.
[35] A.A. Tsyganenko, J. Lamotte, J.P. Gallas, J.C. Lavalley, J. Phys. Chem. 93 (1989) 4179–4183.
[36] B. Klingenberg, M.A. Vannice, Chem. Mater. 8 (1996) 2755–2768.
[37] A. Paulidou, R.M. Nix, Surf. Sci. 470 (2000) L104–L108.
[38] O.V. Manoilova, S.G. Podkolzin, B. Tope, J. Lercher, E.E. Stangland, J.M. Goupil, B.M. Weckhuysen, J. Phys. Chem. B 108 (2004) 15770–15781.
[39] J.C. Lavalley, M. Benaissa, J. Chem. Soc. Chem. Commun. (1984) 908–909.
[40] G. Busca, V. Lorenzelli, V. Sanchez Escribano, R. Guidetti, J. Catal. 131 (1991) 167–177.
[41] V. Sanchez Escribano, G. Garbarino, E. Finocchio, G. Busca, Top. Catal. 60 (2017) 1554–1564.
[42] A. Vazquez, T. Lopez, R. Gomez, X. Bokhimi, A. Morales, O. Novaro, J. Solid State Chem. 128 (1997) 161–168.
[43] A. Vazquez, T. Lopez, R. Gomez, X. Bokhimi, J. Mol. Catal. A: Chem. 167 (2001) 91–99.
[44] G.A.H. Mekhemer, Phys. Chem. Chem. Phys. 4 (2002) 5400–5405.
[45] G. Busca, V. Lorenzelli, Mater. Chem. 7 (1982) 89–126.
[46] J. Lee, H. Jeon, D.G. Oh, J. Szanyi, J.H. Kwak, Appl. Catal. A: Gen. 500 (2015) 58.
[47] W.H. Wade, S. Teranishi, J.L. Durham, J. Phys. Chem. 69 (1965) 590–595.
[48] J. Lee, J. Szanyi, J.H. Kwak, Mol. Catal. 434 (2017) 39–48.
[49] A. Starczewska, R. Wrzalik, M. Nowak, P. Szperlich, Ł. Bober, J. Szala, D. Stróz, D. Czechowicz, Infrared Phys. Technol. 51 (2008) 307–315.
[50] S.C. Street, A.J. Gellman, Colloids Surf. A: Physicochem. Eng. Asp. 105 (1995) 27–34.
[51] H. Wieser, W.G. Laidlaw, P.J. Krueger, H. Fuhrer, Spectrochim. Acta 24A (1968) 1055–1089.
[52] G. Hertzberg, Molecular Spectra and Molecular Structure, Van Nostrand, Princeton, NJ, 1950.
[53] J.F. DeWilde, A. Bhan, Appl. Catal. A Gen. 502 (2015) 361–369.
[54] G.A. Olah, Friedel-Crafts and Relative Reactions vol. 1, Interscience, New York and London, 1963 p. 700.
[55] P. Saenz, R.E. Cachau, G. Seoane, M. Kieninger, O.N. Ventura, J. Phys. Chem. A 110 (2006) 11734–11751.
[56] J.T. Mc Cartney, S. Ergun, Bulletin 641, Bureau of Mines, 1967, p. 29.
[57] I. Stemmler, C. Backles, Absorption Spectroscopy as a Powerful Technique for the Characterization of Single-Walled Carbon Nanotubes, Perkin Elmer, 2013.
[58] Sasol, High Purity Activated Aluminas. http://www.sasoltechdata.com/tds/PURALOX_CATALOX.pdf.
[59] M. Bettman, R.E. Chase, K. Otto, W.H. Weber, J. Catal. 117 (1989) 447–454.
[60] Z. Boukha, L. Fitian, M. López-Haro, M. Mora, J.R. Ruiz, C. Jiménez-Sanchidrián, G. Blanco, J.J. Calvino, G.A. Cifredo, S. Trasobares, S. Bernal, J. Catal. 272 (2010) 121–130.
[61] G. Garbarino, S. Chitsazan, T.K. Phung, P. Riani, G. Busca, Appl. Catal. A: Gen. 505 (2015) 86–97.